Research article

Analysis of corrosion scales formed on steel at high temperatures in hydrocarbons containing model naphthenic acids and sulfur compounds

Peng Jin,[a]* Srdjan Nesic[a] and H. Alan Wolf[b]

Corrosive naphthenic acids and sulfur compounds in crude oils present a major challenge for refineries from a corrosion perspective. Although it is accepted that some sulfur compounds may form protective FeS scales on the metal surface and deter corrosion, attempting to correlate the characteristics of FeS scale with its protective properties has not been successful. Given the complex chemical compositions of real crudes, model sulfur compound and model naphthenic acids were used to mimic the corrosion by crude fractions in the present study. The iron sulfide scale formed by the model sulfur/acid compounds was challenged by naphthenic acids under high-velocity conditions to examine its protectiveness against corrosion. Moreover, the scale was analyzed with transmission electron microscope/energy dispersive X-ray spectroscopy technique, and a layer of iron oxide formed on the 5Cr steel was found when naphthenic acids were present in the solution. The iron oxide layer appeared to be important for maintaining protection against naphthenic acid corrosion, and further analysis revealed that it was composed of magnetite. Copyright © 2015 John Wiley & Sons, Ltd.

Keywords: SEM; TEM; iron oxide; naphthenic acid; high temperature corrosion; model sulfur compound

Introduction

The high content of corrosive naphthenic acids (NAP) and sulfur compounds represents an engineering challenge for refineries that are processing 'opportunity crudes', which are characterized by the ease of procurement and discounted price. However, corrosive species in 'opportunity crudes' may lead to severe corrosion of facilities, which may be mitigated by blending crudes, upgrading materials, and/or adding inhibitors.[1] It is widely accepted that the corrosion from NAP and sulfur compounds takes place via the following reactions:[2]

$$Fe + 2RCOOH \leftrightarrow Fe(RCOO)_2 + H_2 \qquad \text{(Reaction 1)}$$

$$Fe + H_2S \leftrightarrow FeS + H_2 \qquad \text{(Reaction 2)}$$

$$Fe(RCOO)_2 + H_2S \leftrightarrow FeS + 2RCOOH \qquad \text{(Reaction 3)}$$
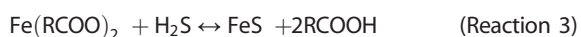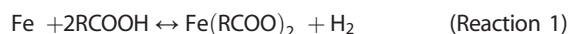
where RCOOH represents a generic NAP, and H_2S represents the sulfur containing compounds in the crude. The iron naphthenates [$Fe(RCOO)_2$] generated in the NAP corrosion (Reaction 1) are oil soluble, and they are removed by the oil flow, whereas the iron sulfide (FeS) generated in (Reaction 2) (sulfidation reaction) is a solid product that is laid down as a scale on the metal surfaces. It is common wisdom in the oil industry that the FeS film may protect the metal against NAP corrosive attack under certain conditions. The two reactions (1 and 2) represent the main corrosive reactions in crude oil, a process that continues because of Reaction 3 when reactive species are regenerated and reintroduced in the corrosive reaction cycle.

To characterize the concentration of NAP in crudes, the TAN or the total acidic number, which is defined as the amount of KOH (in mg) needed to neutralize the acidity in one gram of crude oil, is used in the refining industry.[3] However, the NAP and sulfur compounds in real crudes are very complex, and there are many authors in the literature who focused their studies on crude oil composition. For instance, Dzidic found that a mixture of California crudes possessed NAP ($C_nH_{2n+z}O_2$) with carbon number (n) from 10 to 30 and an index of hydrogen deficiency (z) from 0 to −12.[4] Similar to NAP, the sulfur compounds in the real crudes are complicated and do not always directly relate to the H_2S evolution behavior or crude oils as some authors suggested in their works.[1,5]

The complex composition of crude oil makes it difficult to evaluate accurately its corrosive behavior in laboratory tests.[6,7] Therefore, it is more feasible to investigate the corrosion processes on a lab scale by using model sulfur compounds, and model NAP, dissolved in model oils that can mimic the main characteristic of crude oils and then try to extend the applicability of these results to real crudes. In this project, a model sulfide compound and a commercial NAP mixture were mixed together in a model inert mineral oil, and then they were used to pretreat steel specimens in a stirred autoclave reactor. The corrosion product scale generated in these experiments was subsequently challenged with the NAP mixture in a rotating cylinder autoclave reactor to examine their protectiveness under high temperature and high-velocity conditions.

* Correspondence to: P. Jin, Institute for Corrosion and Multiphase Technology, Chemical and Biomolecular Engineering, Ohio University, 342 West State Street, Athens, OH 45701, USA.
E-mail: pj221108@ohio.edu

a Institute for Corrosion and Multiphase Technology, Ohio University, 342 West State Street, Athens, OH, 45701, USA

b ExxonMobil Research and Engineering Company, 1545 Rt 22E Room LB264, Clinton, NJ, 08801-3095, USA

Table 1. Chemical composition of carbon steel specimen (%wt)

C	Si	Mn	P	S	Cr	Ni	Mo	V	Cu	Fe
0.18	0.41	0.8	0.11	0.06	0.02	0.04	0.02	0.03	0.08	Bal

Table 2. Chemical composition of 5Cr specimen (%wt)

C	Si	Mn	P	S	Cr	Ni	Mo	Cu	Al	Ti	N	Sn	Zr	Fe
0.1	0.24	0.41	0.022	0.005	4.47	0.14	0.5	0.12	0.01	0.006	0.012	0.007	0.002	Bal

Experimental

Experimental materials

To assess the corrosion of the materials used in the field, two of the most commonly utilized steels in refineries were selected for experimentation, that is, the A106 carbon steel (CS, Table 1) and A182-F5 chrome steel (5Cr, Table 2). Steel specimens were in the shape of rings with inner diameter 70.43 mm, outer diameter 81.76 mm, and thickness 5 mm. Before experiments, each specimen was polished with 400 and 600-grit silicon-carbide paper (SiC) in succession. Isopropanol was used to flush specimens during polishing to prevent oxidation and overheating. After polishing, specimens were wiped with a paper towel, rinsed with toluene and acetone, and dried with nitrogen flow. Weights of fresh clean specimens were taken with an analytical balance.

After each experiment, specimens were rinsed with toluene and acetone, gently rubbed with a soft plastic brush, treated with 'Clarke' solution (ASTM G1 – 03),[8,9] and reweighed. Based on the weight difference of specimens before and after the experiment and the exposed surface area, the corrosion rate was calculated.

Experimental solutions

n-dodecyl sulfide (DDS, Fisher Chemical) is an active organosulfur compound which can decompose to H_2S at high temperatures and corrode the steel. For instance, Dettman et al. investigated the corrosion by DDS and other sulfur compounds and their thermolysis at different temperatures.[10] It was found that DDS can undergo decomposition and release H_2S with a yield of 50%, which is higher than most other organosulfur compounds. Therefore, DDS was chosen in the current research to substitute for natural sulfur compounds in crudes.

A commercial NAP mixture with low sulfur content (available from Tokyo Chemical Industry) was selected to mimic natural NAP found in real crudes (Table 3). DDS and/or NAP were dissolved in an inert mineral oil (CITGO, Table 4) to prepare experimental solutions that were later used to pretreat steel specimens. Three different solutions were prepared:

- 'NAP only' consisting of NAP dissolved in mineral oil (TAN = 1.75, S = 0%wt),
- 'DDS only' prepared of DDS dissolved in mineral oil (TAN = 0, S = 0.25%wt), and
- 'DDS + NAP' where both DDS and NAP were dissolved in mineral oil (TAN = 1.75, S = 0.25%wt).

Experimental equipment

Two different experimental setups were used in this research work. The first experimental setup was a stirred autoclave where metal specimens were pretreated with one of the experimental solutions at high temperature under continuous stirring where they were allowed to develop a protective scale. The total volume of the stirred autoclave was 1 l, filled with 0.7 liter of experimental solution. The second experimental setup was a flow-through rotating cylinder autoclave called the high velocity rig (HVR). The HVR was used to investigate the scale tenacity against NAP attack (Fig. 1) under high temperature and high velocity conditions. Specimens pretreated with each of the three different experimental solutions in the stirred autoclave were transferred into the HVR where they were exposed to the mineral model oil containing the model NAP at TAN 3.5 (the challenge solution). The HVR was designed to create a high flow velocity and associated turbulence and shear stress. The core of the HVR system was the reactor, or autoclave with a rotating cylinder setup that enabled flow through of the NAP solution. As shown in Fig. 2, specimens were stacked together in the HVR reactor, and only the outer surface was exposed to the challenge solution.

Experimental procedures

The experimental procedure consisted of two consecutive steps:

1) 'Pretreatment' – generation of scale in the stirred autoclave. CS and 5Cr specimens were pretreated in the stirred autoclave with one of the three experimental solutions that generated corrosion scales on the full specimen surface. Prior to the

Table 3. Boiling point range of the commercial naphthenic acids mixture

Parameter	Temperature (℃)
Initial boiling point	239
50%	296
Final boiling point	493

Table 4. Selected physical and chemical properties of the mineral oil

Parameter	Description
Appearance	Clear liquid
Color	Colorless
Odor	Odorless
Density (at 16 ℃, kg/m^3)	876
Flash point (℃)	254
Average molecular weight	530
Initial boiling point (℃)	388
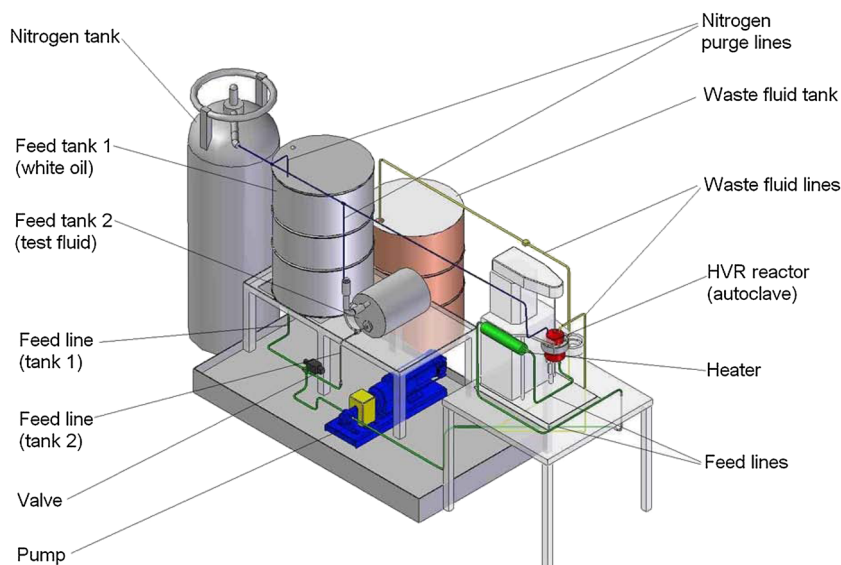
Figure 1. Schematic rendering of the high velocity rig used in the 'challenge' experiment.

starting of pretreatment, the stirred autoclave was purged with nitrogen gas to remove oxygen. During the pretreatment, stagnant specimens were fully immersed in the experimental solution, which was stirred (500 rpm) to enhance heat transfer. The pretreatment temperature was 316 °C (600 °F), and the duration was 24 h. The stirred autoclave was pressurized by the autogenous gas released by the experimental solution.

2) 'Challenge' – evaluation of scale protectiveness in the HVR. After pretreatment in the stirred autoclave, the specimens were transferred into the HVR, which was fed with the challenge solution of NAP acid in mineral oil (TAN = 3.5, S = 0% wt). The challenge temperature was 343 °C (650 °F), and the duration was 24 h. During the challenge, the speed of the rotating cylinder was set to 2000 rpm (translating to a peripheral velocity of 8.5 m/s, Reynolds number of 1771 and wall shear stress of 74 Pa). A back-pressure of 150 psig was applied to suppress breakout of gas; flow-through rate of the oil containing fresh NAP was set to 7.5 cm^3/min. In addition to the high-TAN value of the challenge solution, the high peripheral velocity helped to create a corrosive condition and to investigate the scale protectiveness.

Further specimen investigation focused on analyzing the structure and chemical composition of the scales using a scanning electron microscopy (SEM) and focused ion beam/transmission electron microscopy (FIB/TEM) combined with energy dispersive X-ray spectroscopy (EDS) as well as convergent beam electron diffraction (CBED).

Evaluation of corrosion rates

Corrosion rates of specimens were calculated based on their weight loss during the experiment. For the pretreatment experiment conducted in the stirred autoclave, the corrosion rate was calculated using Eqn (1).

$$CR_{Pretreatment} = \frac{(IW - FW)}{\rho_{steel} \times A_{s,Pretreatment} \times t_{Pretreatment}} \times 10 \times 24 \times 36 \quad (1)$$

where
$CR_{Pretreatment}$ – Pretreatment corrosion rate (mm/y)
IW – Initial weight of fresh polished steel specimen (g)
FW – Final weight of steel specimen after treated with Clarke solution (g)
ρ_{steel} – Density of steel specimen, (g/cm^3)
$A_{s, Pretreatment}$ – Area of steel specimen exposed to corrosive fluid during pretreatment (cm^2)
$t_{Pretreatment}$ – Duration of experimentation in the autoclave (h)

In a combined pretreatment-challenge experiment, fresh polished specimens were pretreated in the autoclave followed by challenging in the HVR. While the corrosion rate in the pretreatment step could be calculated according to Eqn (1), the challenge corrosion was assessed by using the following equation

$$CR_{Challenge} = \frac{(IW - FW - WL_{Pretreatment})}{\rho_{steel} \times A_{s,Challenge} \times t_{Challenge}} \times 10 \times 24 \times 36 \quad (2)$$

where
$CR_{Challenge}$ – Net corrosion rate from the challenge phase (excluding the autoclave phase) (mm/y)
IW – Initial weight of fresh polished steel specimen (g)
FW – Final weight of steel specimen after treated with Clarke solution (g)
$WL_{Pretreatment}$ – Weight loss of specimen in the pretreatment phase (g)ρ_{steel} – Density of steel specimen (g/cm^3)
$A_{s, Challenge}$ – Area of steel specimen exposed to corrosive fluid during challenge (cm^2)
$t_{Challenge}$ – Duration of experimentation in the HVR (h)

For each metallurgy (CS or 5Cr steel), three ring specimens were used in the experiment and the corrosion rate of each specimen was calculated according to Eqn (1) or (2).

Results

The following paragraphs present and discuss the experimental data for the 'pretreatment experiments' (where scales were

(a)

(b)
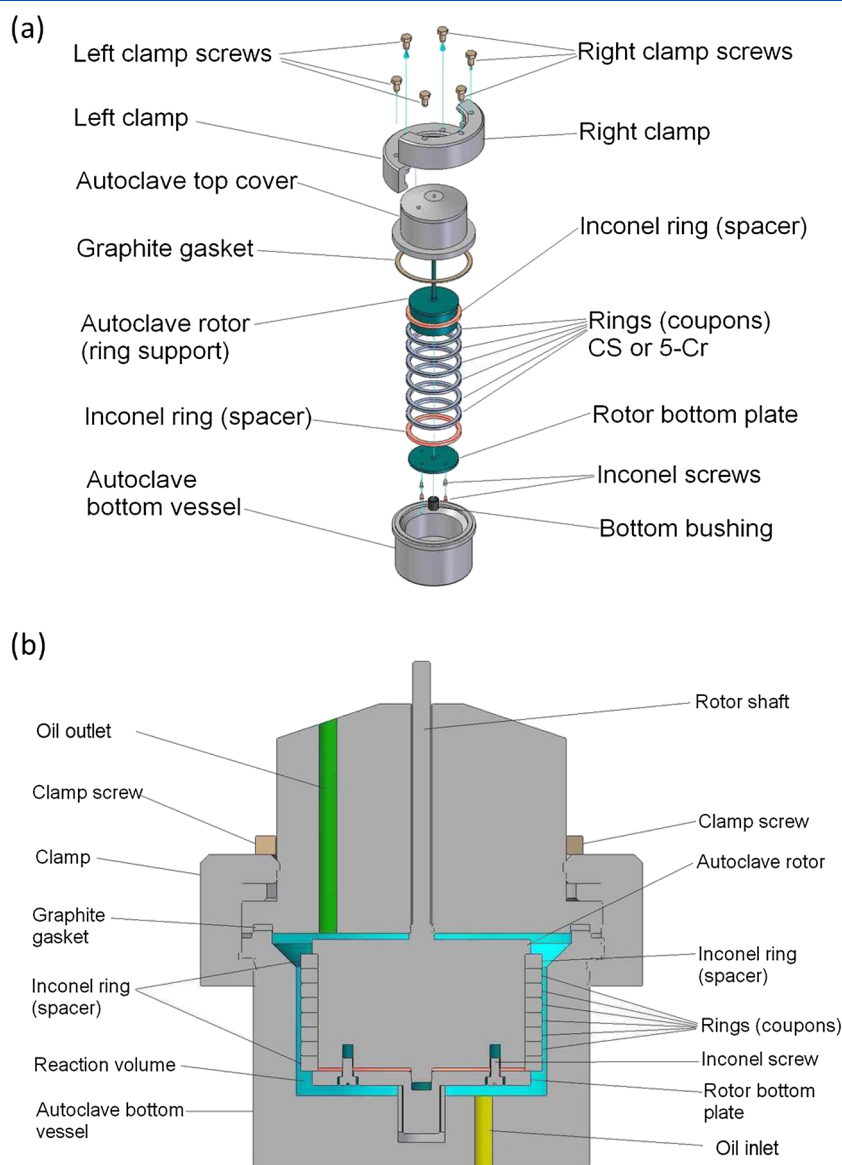
Figure 2. Scheme of high velocity rig reactor. (a) Exploded view and (b) Cross-section view.

Table 5. Pretreatment corrosion rates for carbon steel and 5Cr at 316 °C (600 °F)

Pretreatment solution	Pretreatment corrosion rate (mm/y)	
	CS	5Cr
NAP only *TAN 1.75, S = 0%wt*	0.3	0.2
DDS only *TAN 0, S = 0.25%wt*	0.2	0.1
DDS + NAP *TAN 1.75, S = 0.25%wt*	0.2	0.2

generated in the stirred autoclave) and the 'pretreatment-challenge' experiments (where scales generated in the stirred autoclave were subsequently challenged in the HVR). Generally, experiments were not repeated except some critical ones.

Pretreatment experiment results

Scales were formed in pretreatment experiment on CS and 5Cr specimens using one of the experimental solutions described in previous paragraphs. Table 5 compares the corrosion rates for CS and 5Cr specimens pretreated at 316 °C (600 °F) with the three different experimental solutions prepared by using the model compounds. The two types of steel showed similar pretreatment corrosion rates in each of the solutions. Generally, the presence of 5% chromium in the steel did not lower the pretreatment corrosion rates significantly.

Challenge experiment results

In the next step, a new set of specimens that was pretreated in the stirred autoclave with each of the three experimental solutions was subsequently transferred into the HVR. Specimens were exposed to air during the transfer from the pretreatment

Table 6. Challenge corrosion rates for carbon steel and 5Cr pretreated with three solutions

Pretreatment solution	Challenge corrosion rate (mm/y)	
	CS	5Cr
NAP only *TAN 1.75, S = 0%wt*	7.9	0
DDS only *TAN 0, S = 0.25%wt*	6.8	1.6
DDS + NAP *TAN 1.75, S = 0.25%wt*	2.5	0.3
Pure TAN 3.5 corrosion rate	7.8	1.8

(in the stirred autoclave) to the challenge (in the HVR). The time of exposure was less than 5 min. Moreover, during the transfer, the specimen surface was still covered by the experimental solution used in the pretreatment. In preliminary experimentation, this procedure was examined by varying the duration of the transfer process, and it was found that it did not significantly impact the results

The HVR was fed with the 'challenge' solution of NAP dissolved in mineral oil (at TAN 3.5). The challenge corrosion rates for CS and 5Cr are shown in Table 6. For CS specimens pretreated in 'NAP only' solution, the challenge corrosion rates were high and close to CS 'pure TAN 3.5 corrosion rate'. 'Pure TAN 3.5 corrosion rate' refers to the baseline corrosion rate of fresh polished specimens with no surface scale that were installed in the HVR and were corroded by the TAN 3.5 solution. Also, the scale formed in 'DDS only' solution on CS showed little protection against NAP challenge. The most protective scale for CS was generated in the 'DDS + NAP' solution, and its challenge corrosion rate was reduced to one-fourth of the 'pure TAN 3.5 corrosion rate'.

Generally, the 5Cr specimens showed lower challenge corrosion rates than those of CS. Similarly, the scale formed in 'DDS only' solution on 5Cr was not protective (the challenge corrosion was 1.6 mm/y) unless NAP was added to the solution (the challenge corrosion rate was reduced to 0.3 mm/year). However, the most striking finding was that 5Cr specimens pretreated in 'NAP only'

solution gave a zero challenge corrosion rate (0 mm/year), which contradicted the traditional theory on NAP corrosion. This experiment was repeated four times, and the same challenge corrosion rate was confirmed each time. It seemed that there was 'something' formed on the steel surface protecting the steel from attack by NAP which was not expected in the absence of DDS and therefore, microscopy analysis on the metal surface was performed to explain the unexpected protection of scale.

Scanning electron microscopy/energy dispersive X-ray spectroscopy analysis

The scales formed on steel specimens were analyzed first using the SEM combined with EDS. Low corrosion rates of 5Cr specimens obtained during the challenge experiments suggested that the scales formed on this type of steel were protective against NAP attack even in the absence of sulfur containing compounds (DDS). Therefore, the following paragraphs will focus mainly on analysis of the unexpected results generated using the 5Cr specimens.

Figure 3 shows the cross-section of 5Cr specimens after pretreatment in the three solutions described previously. By visual examination, the 'NAP only' solution seemed to have left nothing detectable on the steel surface, which was confirmed by EDS analysis. However, the challenge experimentation indicated that the 5Cr specimen seen in image in Fig. 3a was most resilient in the harsh condition of the TAN 3.5 challenge (Table 6). Therefore, it was concluded that the SEM/EDS surface analysis was not helpful in explaining the low challenge corrosion rate of the 5Cr specimen. On the other hand, multiple layers were formed in 'DDS only' solution, and chromium was found in the inner layer, which was covered by an FeS layer (Fig. 3b and e). In the 'DDS + NAP' solution, the layer of FeS was still observed on the specimen surface as shown by image in Fig. 3c and f; however, the corresponding challenge corrosion rate was lower (Table 6).

The 5Cr specimen surface after 'challenge' is shown in Fig. 4. The 5Cr specimen pretreated with 'NAP only' solution gave a zero challenge corrosion rate (Table 6), but no obvious layer was found
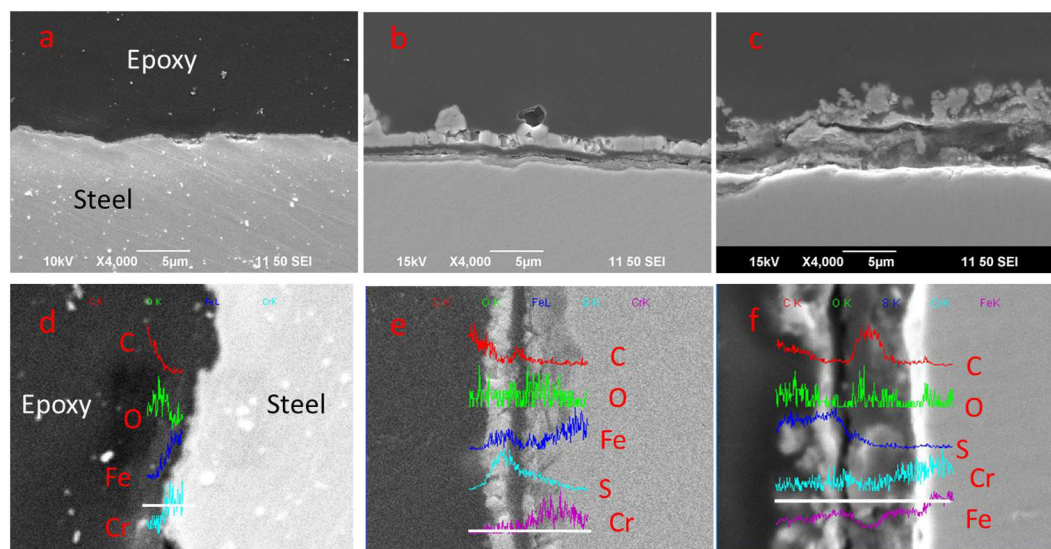
Figure 3. Cross-section scanning electron microscopy images of 5Cr specimens pretreated with (a) 'NAP only' solution, (b) 'DDS only' solution, and (c) 'DDS + NAP' solution, at 316 ℃ (600 °F). Bottom images (d), (e), and (f) show corresponding EDS analyses of the scales. The energy dispersive X-ray spectroscopy analysis was performed along the white line shown on the bottom of the image.
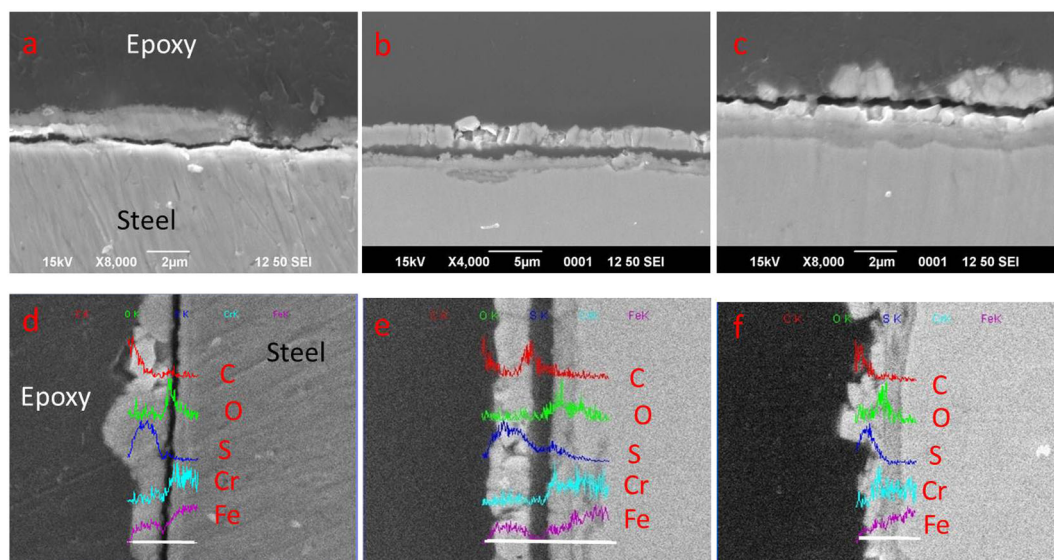
Figure 4. Cross-section scanning electron microscopy images of 5Cr specimens pretreated with (a) 'NAP only' solution, (b) 'DDS only' solution, and (c) 'DDS + NAP' solution, at 316 °C (600 °F); challenged with naphthenic acids solution (TAN 3.5) at 343 °C (650 °F). Bottom images (d), (e), and (f) show corresponding energy dispersive X-ray spectroscopy analyses. The energy dispersive X-ray spectroscopy analysis was performed along the white line on the bottom of the images.

through SEM analysis (Fig. 3). After 'challenge', a continuous layer was still not visible. However, EDS analysis showed a peak of oxygen in image (Fig. 4d) and suggested that there might be a thin oxide layer, and further analysis was necessary for verification. The unprotective layer formed in 'DDS only' solution was characterized by delaminated layers and flakes of FeS as shown in images in Fig. 4b and e. For the scale formed in 'DDS + NAP' solution, seen in images in Fig. 4c and f, the layer of FeS was also observed after challenge, but the 'challenge' corrosion rate was only one-fourth of 'pure TAN 3.5 corrosion rate' for 5Cr.

It is noteworthy that the most intensive peak of oxygen appeared in the EDS analyses for the two specimen, which had the more protective properties of the surface scale layer. However, the SEM/EDS analysis was not sufficiently powerful to provide submicron resolution and fully reveal the structure of thin surface layer, which seemed to be the key to the corrosion protection. An analytical technique offering a higher resolution was needed, and in this case the FIB/TEM/EDS and CBED were used for more in-depth analyses.

Transmission electron microscopy/energy dispersive X-ray spectroscopy analysis

To find the explanation for the protectiveness of scales formed in different solutions, combined FIB/TEM/EDS analyses[11] were conducted on 5Cr specimens pretreated in 'DDS only' solution, 'DDS + NAP' solution, and 'NAP only' solutions. The scales formed in these three solutions are shown in Fig. 5 (cross-section TEM image). Two delaminated layers were observed for the 'DDS only' solution, which is consistent with the SEM image shown in Fig. 3b. The outer layer formed in 'DDS + NAP' solution was more intimately attached to the inner layer (Fig. 5b). The total layer thickness was about 1 μm while the inner layer accounted for less than half of that. A thin scale with a thickness of 165 nm was formed on the 5Cr specimen pretreated in the 'NAP only' solution (Fig. 5c), which showed the lowest challenge corrosion rate (Table 6).

According to the EDS analysis shown in Fig. 6a, FeS was the major component in the inner layer formed in the 'DDS only' solution, although there was a minor amount of oxygen, which may be
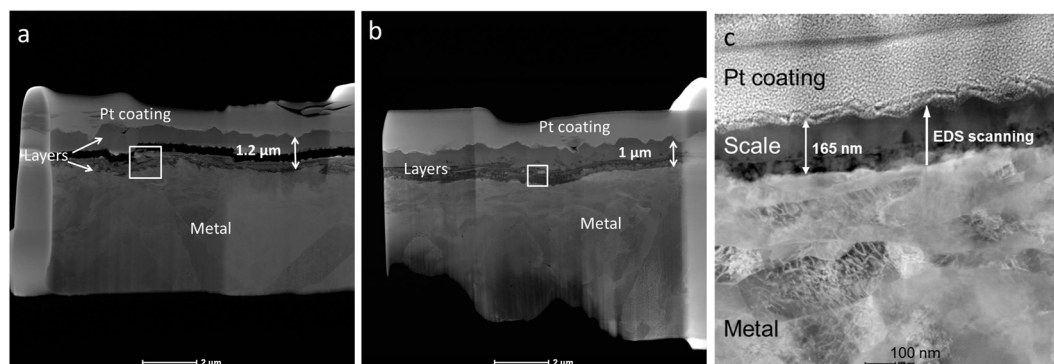
Figure 5. Transmission electron microscopy image of 5Cr specimen pretreated with 'DDS only' solution (a), 'DDS + NAP' solution (b), and 'NAP only' solution (c) at 316 °C (600 °F).
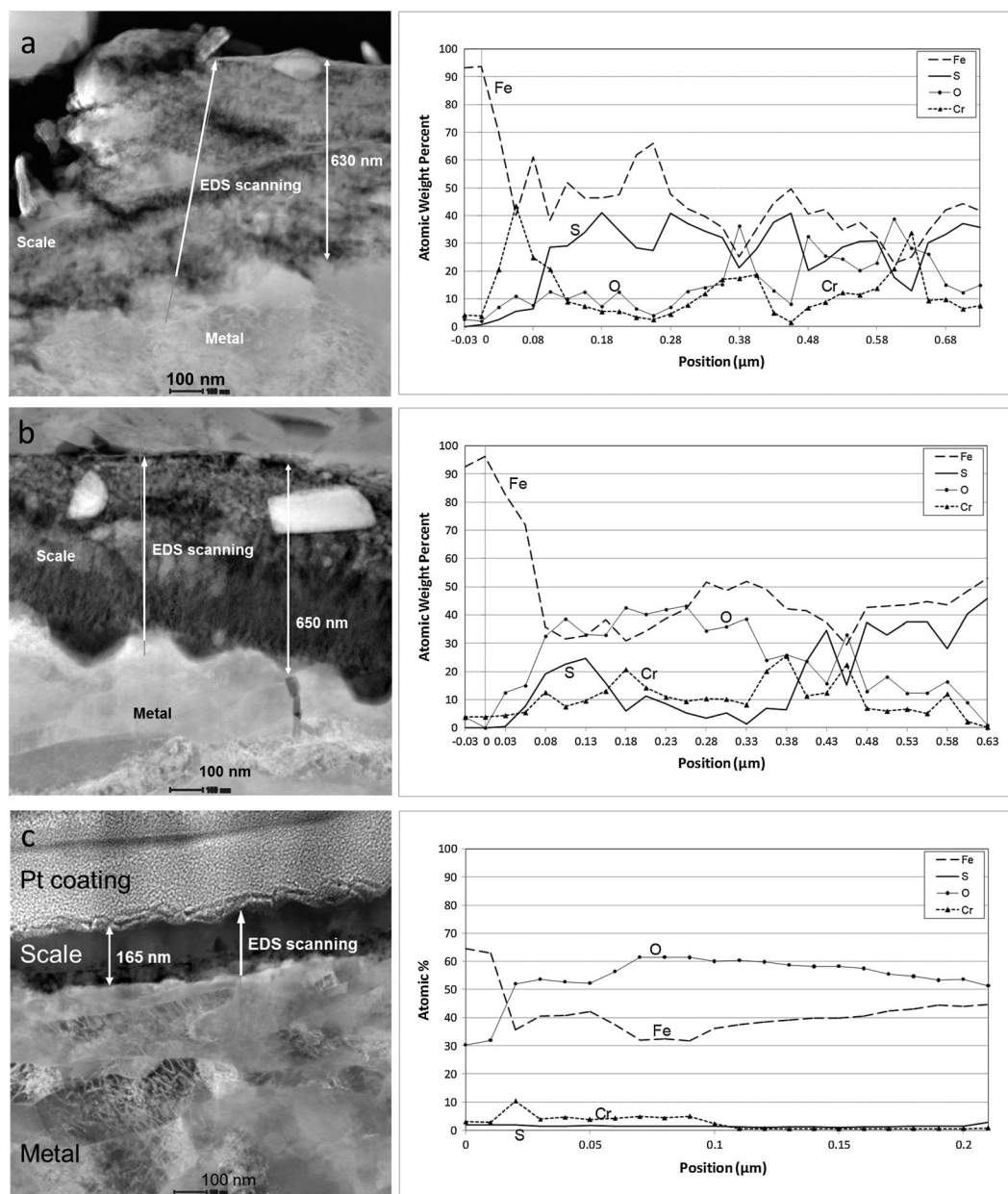
Figure 6. Transmission electron microscopy image and energy dispersive X-ray spectroscopy analysis on the inner layer of 5Cr specimen pretreated with 'DDS only' solution (a), 'DDS + NAP' solution (b), and 'NAP only' solution (c) at 316 °C (600 °F). The elemental data were collected along the white line (from the bottom to the top) indicated on the transmission electron microscopy image.

due to sample oxidation or contamination. About 5% of chromium showed up in the substrate steel, which was consistent with the chromium content in 5Cr steel. The EDS analysis of the scale formed in 'DDS + NAP' solution on 5Cr indicated that the chemical composition of the scale inner layer changed (Fig. 6b). The primary difference in chemical composition of the scales is that a considerable amount of sulfur in Fig. 6a is replaced by oxygen in Fig. 6b. In Fig. 6b, the oxygen content is over 40% while the sulfur amount decreases to values lower than 5%. Similar to Fig. 6a, the chromium concentration in Fig. 6b increases from 5% in the steel substrate to about 10% in the inner scale layer (enrichment). Given that the outer layer was composed of FeS in both cases (for 'DDS only' and the 'NAP + DDS' pretreatments), the difference in the protective properties of scale is most likely related to the oxygen content found in the inner layer.

Figure 6c shows TEM/EDS analysis on the most protective scale formed in the 'NAP only' solution on 5Cr. Compared with the scale formed in 'DDS only' and 'DDS + NAP' solutions, the scale was composed of only one layer. The EDS analysis reveals that the scale was composed of iron and oxygen, although trace amounts of chromium and sulfur were found. The chromium could be traced back to the 5Cr and sulfur could either be from the trace amounts contained in the commercial NAP blend used and/or from the slight contamination of the stirred autoclave. CBED analysis was performed and it was found that magnetite (Fe_3O_4) was the major component of the oxide layer (Fig. 7). Scales formed in three solutions are compared in Table 7.

It is concluded that the magnetite formed in the 'NAP only' solution was protecting the steel from the challenge attack by the NAP.
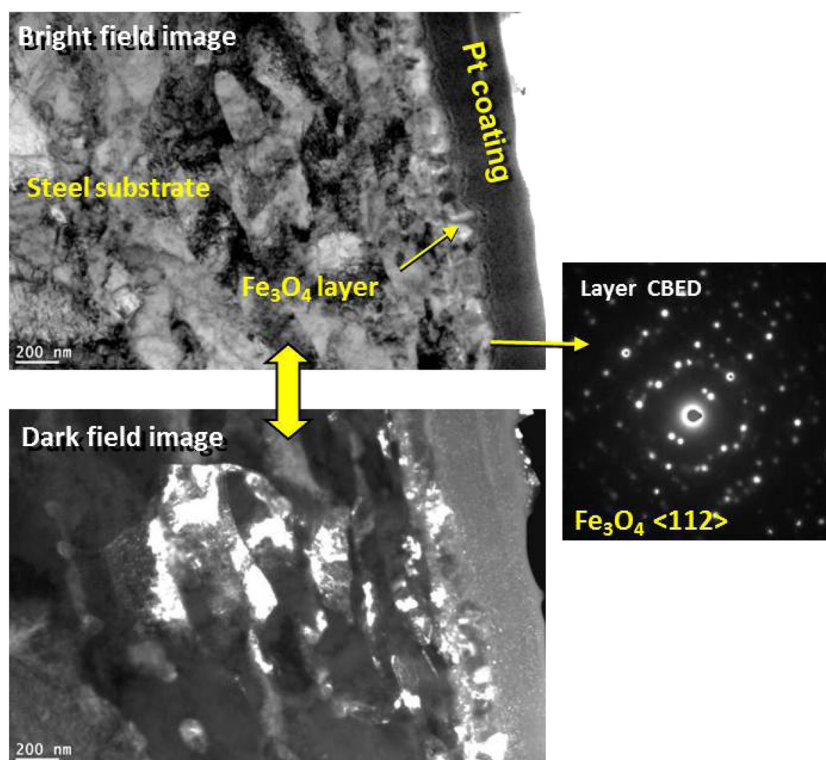
Figure 7. Transmission electron microscopy images and convergent beam electron diffraction pattern of layer formed in 'NAP only' solution at 316 °C (600 °F) for 5Cr specimen.

Table 7. Comparison of scales on 5Cr specimen pretreated with 'NAP only' solution, 'DDS only' solution, and 'DDS + NAP' solution at 316 °C (600 °F)

Pretreatment solution	TAN	Sulfur content	Scale characterization	
			Thickness	Component
NAP only	1.75	0	165 nm	Iron oxide
DDS only	0	0.25%wt	Outer scale: 630 nm	Outer scale: iron sulfide
			Inner scale: 670 nm	Inner scale: iron sulfide
DDS + NAP	1.75	0.25%wt	Outer scale: 650 nm	Outer scale: iron sulfide
			Inner scale: 670 nm	Inner scale: iron oxide

Discussion

The corrosion of steel in the presence of model NAP or sulfur compounds was extensively studied based on the perception that FeS was the major cause of corrosion protection. For instance, Craig coined the term 'naphthenic acid corrosion index (NACI)', trying to predict the protection of FeS.[12] Turnbull *et al.* attributed the decrease of corrosion rates to the presence of FeS and the adsorption of NAP, despite the observation of corrosion product on the steel surface after the NAP corrosion.[13] However, in a long term study involving many different crude fractions as well as model oil systems, it was shown that the morphology or the weight of FeS was not correlated to its protection.[6]

On the other hand, the formation of an iron oxide or magnetite layer relating to NAP corrosion was reported previously in the literature. Kamel *et al.* noted that an iron oxide layer was revealed by XRD and XPS analysis on steel specimens corroded by crude fractions in the autoclave.[14] However, it was postulated that iron oxide existed in the outermost layer and resulted from sample oxidation

after the test. Smart *et al.* found the existence of magnetite and minor amount of hematite (α-Fe_2O_3) and pyrrhotite ($Fe_{(1-x)}S$) on CS surface after testing with a high-TAN crude.[15] The layer of magnetite was suspected to be protective, but the role of NAP in the formation of iron oxide layer was not considered. Magnetite was also found in experiments by Huang *et al.*[16] by using model sulfur compound (dimethyl disulfide) and NAP. Again, the appearance of magnetite was considered to be the result of contamination and sulfide layer oxidation.

Our current research clearly showed that presence of NAP was necessary to form the oxide layer which was protective against NAP corrosion. The FeS scale formed in the sulfur-only containing solution (in the form of DDS), was not protective. It is different from the commonly accepted viewpoint that the FeS scale is protective.

Before the pretreatment, the solution was purged with nitrogen to remove oxygen and to create a reductive condition. It is here further postulated that the formation of the oxide scale is due to the decomposition of iron naphthenates, $Fe(RCOO)_2$. In fact, the decomposition of iron naphthenates between 200 °C and 800 °C was

Table 8. Pretreatment and challenge corrosion rates for 5Cr in the first and second repeat experiment

Experiment	Corrosion rate (mm/y)	
	Pretreatment	Challenge
First repeat		
Six ring specimens	0.2	0.1
Second repeat		
Two ring specimens	0.5	0.2

reported first in 1976, and magnetite was one of the products.[17] Moreover, decomposition of ferrous carboxylates is widely used in the preparation of nano-scale magnetite.[18] Investigation of the reaction mechanism suggested that wüstite (FeO) was the initial product and would disproportionate to magnetite.[14] Therefore, the following reaction sequence might explain the formation of the magnetite layer during the process of NAP corrosion of steel.[18–20]

$$Fe(RCOO)_2 = FeO + CO_2 + RCOR \qquad \text{(Reaction 4)}$$
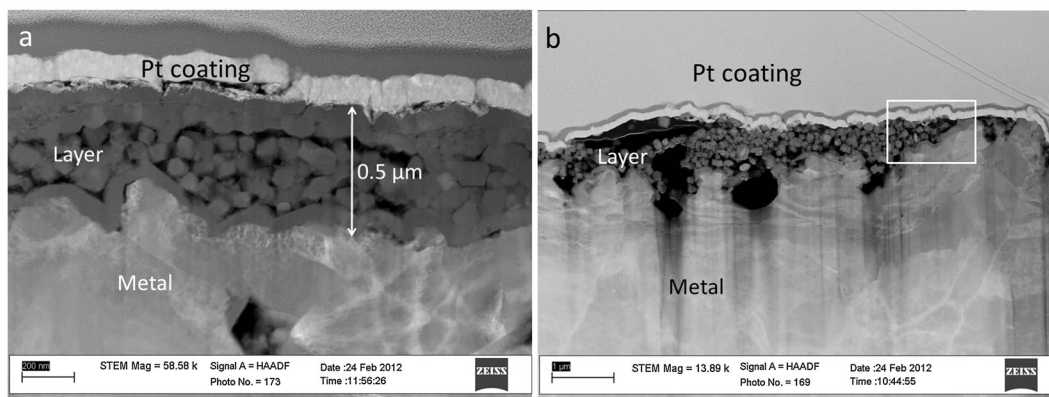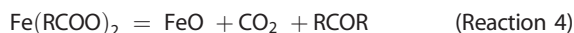
Figure 8. Transmission electron microscopy images of 5Cr steel specimen pretreated with the 'NAP only' solution at 316 °C (600 °F) for 24 h in the first repeat experiment (a) and the second repeat experiment (b).
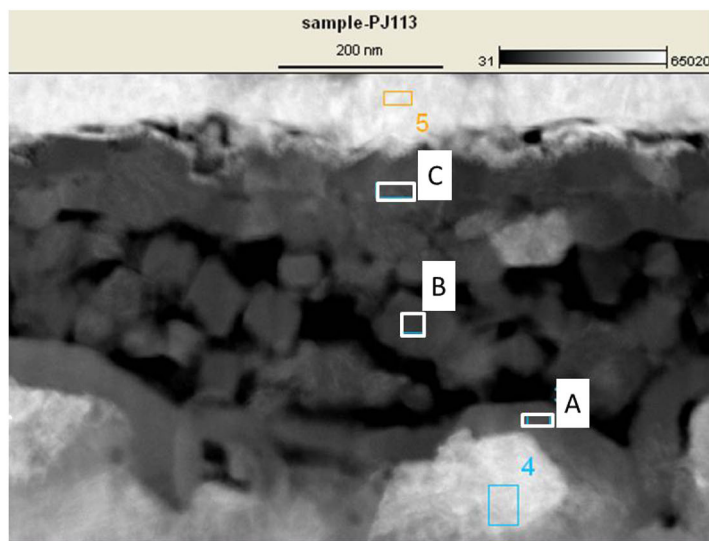
A	
Element	Atomic%
O	70.19
Fe	29.81

B	
Element	Atomic%
O	67.93
S	0.84
Fe	30.60
Cr	0.27

C	
Element	Atomic%
O	48.98
S	0.58
Fe	48.39
Cr	1.52

Figure 9. Energy dispersive X-ray spectroscopy analysis on selected areas of the layer shown in Figure 8a.
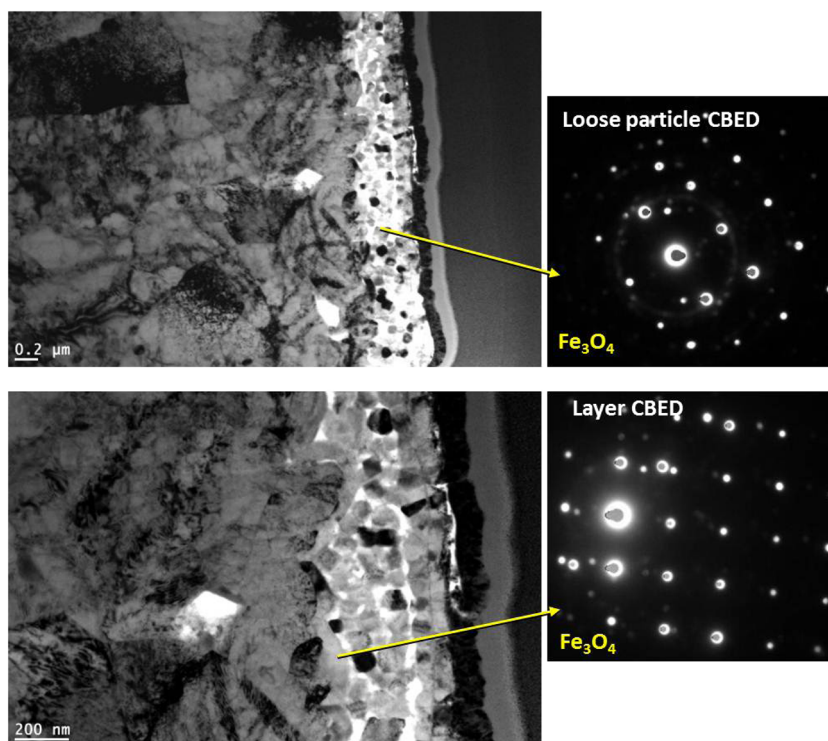
Figure 10. Transmission electron microscopy images and convergent beam electron diffraction pattern of the continuous layer and the crystalline particle shown in Figure 8a.

$$4FeO = Fe_3O_4 + \alpha\text{-}Fe \qquad \text{(Reaction 5)}$$

The very thin layer of magnetite is of crucial importance when considering the protectiveness of corrosion product scales found in high temperature corrosion of steel in refinery conditions.

To verify the hypothesis relating to the role of iron naphthenates, the pretreatment-challenge experimentation involving the 'NAP only' solution was repeated. In the first repeat experiment, the pretreatment was done exactly the same – with six ring specimens (three made of CS and three made of 5Cr steel) in the stirred autoclave. The second 'repeat' experiment followed the same procedure except that only two ring specimens which were made of 5Cr steel were pretreated in the stirred autoclave. According to the hypothesis, lesser amount of iron oxide should be observed on specimens in the second repeat experiment due to the lower concentration of iron naphthenates generated in the pretreatment.

Table 8 summarizes the pretreatment and challenge corrosion rates for the repeat experiments. Given that the fluid in the stirred autoclave was not replenished, the pretreatment with a fewer number of specimens lead to a higher pretreatment corrosion rate. However, layers formed in both repeat experiments were protective, as shown by the challenge corrosion rates. Note that the pretreatment corrosion rate in the second repeat experiment is even higher than the challenge corrosion rate.

The TEM image for the 5Cr specimen after pretreatment in the first experiment reveals a total layer thickness of 0.5 μm (Fig. 8a). Interestingly, an attached inner layer of ~50 nm is observed to follow the profile of the metal surface with compact crystalline particles above it in the outer layer. EDS analysis indicates that both the continuous inner layer and crystalline particles in the outer layer are
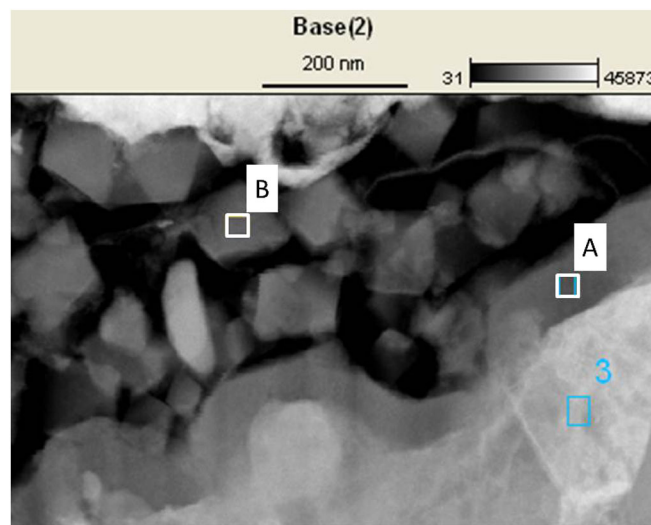
A

Element	Atomic%
O	60.54
S	0.70
Fe	38.77

B

Element	Atomic%
O	47.58
S	3.80
Fe	47.77
Cr	0.84

Figure 11. Energy dispersive X-ray spectroscopy analysis on selected areas of the layer shown in the rectangle of Figure 8b.
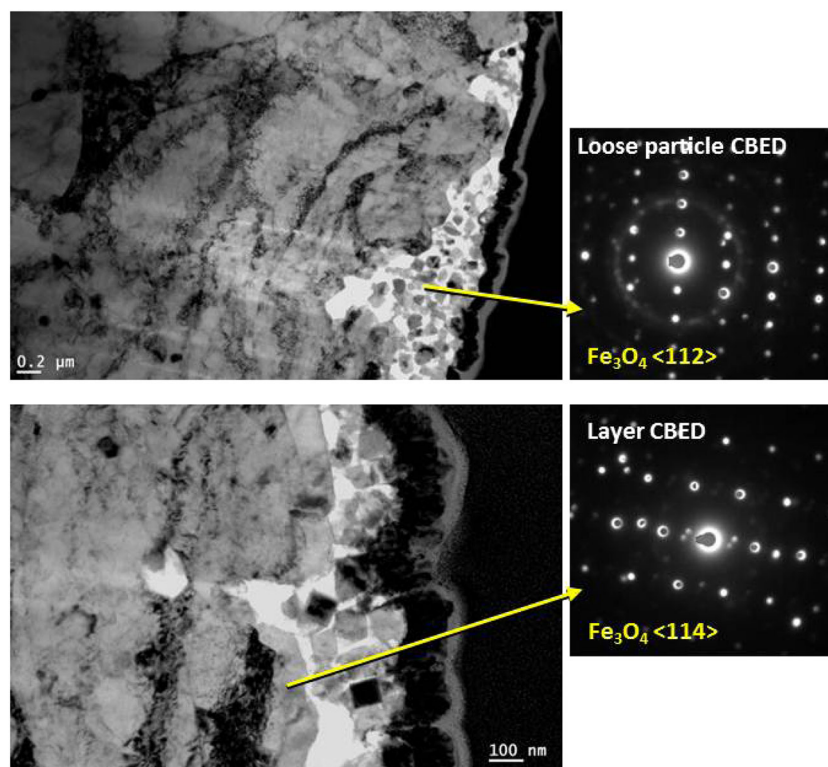
Figure 12. Transmission electron microscopy images and convergent beam electron diffraction pattern of the continuous layer and the crystalline particle shown in Figure 8b.

composed of iron oxide (Fig. 9), which is consistent with results shown in Fig. 6c. Moreover, the oxygen is not evenly distributed in the two layers. The oxygen content in the inner layer is as high as ~70% while it decreases to ~50% in the outer layer. Trace amount of chromium and sulfur are observed only in the outer layer while the inner layer is composed of iron and oxygen exclusively. However, CBED analysis suggests that both the continuous layer and the crystalline particles in the outer layer are composed of magnetite (Fig. 10). It is the magnetite layer that is protecting the 5Cr steel.

In the second experiment, the profile of the metal surface suggests the initiation of pitting corrosion (Fig. 8b). Lesser amount of the corrosion product formed when there was less amount of metal in the autoclave. This phenomenon may be due to the fact that smaller amount of iron naphthenates was released. Nevertheless, a protective and continuous layer (~50 nm) is observed again, which is consistent with the finding in Fig. 8a.

Figure 11 reveals a consistent elemental profile as in Fig. 9. The oxygen content in the inner layer is higher than that of crystalline particles in the outer layer. Chromium is found only in the crystalline particles rather than in the inner layer. Obviously, the low challenge corrosion rate should be correlated with the inner layer rather than the loose crystalline particles in the outer layer. Again, it is implied that the protective properties of the corrosion product layers are determined primarily by the thin inner layer of iron oxide rather than the thicker outer corrosion product layer. CBED reveals the presence of magnetite in the corrosion product (Fig. 12).

Figures 11 and 12 show that crystalline particles of magnetite accumulate in cavities while they seem to be uniformly distributed on the metal surface, as illustrated in Fig. 8a. This phenomenon could be explained by the difference in concentrations of iron naphthenates, which would decompose to form iron oxide. With

a high concentration of iron naphthenates in the first experiment, the inner oxide layer was formed quickly and crystalline particles of iron oxide deposited on the uniformly corroded metal surface. On the other hand, when the concentration of iron naphthenates was as low as in the second experiment, iron oxide could only crystallize in cavities where the concentration of iron naphthenates was higher than the bulk fluid. These experiments reinforced the hypothesis that the iron oxide was formed due to the decomposition of iron naphthenates.

However, the role of chromium on the layer protectiveness is not very clear. Layers formed on 5Cr steel specimens are generally more protective than those on CS specimens. It implies that the chromium, despite its low content, is the crucial factor which enhances the layer protectiveness. It could act as a 'catalyst' to promote the formation of magnetite. By replacing some iron atoms in the magnetite, chromium may make the layer more chemically stable. This mechanism is still unclear and deserves further investigation.

Conclusions

1) The FeS scale, formed because of the sulfur content in the oil, was not directly correlated to the reduction of NAP corrosion.
2) Having NAP in the oil improved the protectiveness of the surface scales, especially for 5Cr steel.
3) A thin submicron oxide layer, which was protective against NAP corrosion, was found by using FIB/TEM combined with EDS analysis. Its formation was clearly related to the presence of NAP in the oil. By using CBED, it was found that the oxide layer was composed of magnetite.
4) It is hypothesized that decomposition of iron naphthenates resulted in the formation of the magnetite layer and

chromium played an important role in this process. Further experimental and analytical work should focus on the verification of this mechanism.

References

[1] S. D. Kapusta, A. Ooms, A. Smith, F. Van den Berg, W. Fort, CORROSION/ 2004, March 28–April 1, **2004**, Houston, Texas, paper no. 04637.

[2] E. Slavcheva, B. Shone, A. Turnbull, *Brit. Corros. J.* **1999**, *34*, 125.

[3] ASTM D664: Standard Test Method for Acid Number of Petroleum Products by Potentiometric Titration, Annual Book of ASTM Standards, West Conshohocken, PA, **1990**, vol. 05.01.

[4] I. Dzidic, A. C. Somerville, J. C. Raia, H. V. Hart, *Anal. Chem.* **1988**, *60*, 1318.

[5] R. D. Kane, M. S. Cayard, *MP*, **1999**, *38*, 48.

[6] G. M. Bota, D. Qu, S. Nesic, H. A. Wolf, CORROSION/2010, March 14 – 28, **2010**, San Antonio, Texas, paper no. 10353.

[7] G. M. Bota, S. Nesic, CORROSION/2013, March 17–21, **2013**, Orlando, Florida, paper no. 2512.

[8] ASTM G1 - 03 (2011): Standard Practice for Preparing, Cleaning, and Evaluating Corrosion Test Specimens, Annual Book of ASTM Standards, West Conshohocken, PA, **2011**, vol. 03.02.

[9] S. G. Clarke, *Trans. Electrochem. Soc.* **1936**, *69*, 131.

[10] H. D. Dettman, N. Li, D. Wickramasinghe, J. Luo, *NACE 2010 Northern Area Western Conference*, February 15-18, **2010**, Calgary, Alberta, Canada.

[11] D. G. Stroppa, L. F. Zagonel, L. A. Montoro, E. R. Leite, A. J. Ramirez, *Chemphyschem.* **2012**, *13*, 437.

[12] H. L. Craig, CORROSION/1995, March 21-23, **1995**, Houston, Texas, paper no. 333.

[13] A. Turnbull, E. Slavcheva, B. Shone, *Corr.* **1998**, *54*, 922.

[14] M. El Kamel, A. Galtayries, P. Vermaut, B. Albinet, G. Foulonneau, X. Roumeau, B. Roncin, P. Marcus, *Surf. Interface Anal.* **2010**, *42*, 605.

[15] N. R. Smart, A. P. Rance, A. M. Pritchard, CORROSION/2002, March 7-12, **2002**, Denver, Colorado, paper no. 02484.

[16] B. S. Huang, W. F. Yin, D. H. Sang, Z. Y. Jiang, *Appl. Surf. Sci.* **2012**, *259*, 664.

[17] J. Fukushima, K. Kodaira, T. Matsushita, *J. Ceram. Soc. Jpn.* **1976**, *84*, 529.

[18] F. X. Redl, C. T. Black, G. C. Papaefthymiou, R. L. Sandstrom, M. Yin, H. Zeng, C. B. Murray, S. P. O'Brien, *JACS.* **2004**, *126*, 14583.

[19] S. Stolen, R. Gloeckner, F. Gronvold, *Thermochim. Acta.* **1995**, *256*, 91.

[20] P. Jin, H. A. Wolf, S. Nesic, CORROSION/2014, March 9-13, **2014**, San Antonio, Texas, paper no. 4075.